



HAL
open science

Local investigation of the emissive properties of LaB₆-ZrB₂ eutectics

Marie-Hélène Berger, T. C. Back, P. Soukiassian, D. Martinotti, L. Douillard,
S. B. Fairchild, J. J. Boeckl, V. Filipov, A. Sayir

► **To cite this version:**

Marie-Hélène Berger, T. C. Back, P. Soukiassian, D. Martinotti, L. Douillard, et al.. Local investigation of the emissive properties of LaB₆-ZrB₂ eutectics. *Journal of Materials Science*, 2017, 52, pp.5537-5543. 10.1007/s10853-017-0816-0. cea-01484778

HAL Id: cea-01484778

<https://cea.hal.science/cea-01484778>

Submitted on 7 Jun 2017

HAL is a multi-disciplinary open access archive for the deposit and dissemination of scientific research documents, whether they are published or not. The documents may come from teaching and research institutions in France or abroad, or from public or private research centers.

L'archive ouverte pluridisciplinaire **HAL**, est destinée au dépôt et à la diffusion de documents scientifiques de niveau recherche, publiés ou non, émanant des établissements d'enseignement et de recherche français ou étrangers, des laboratoires publics ou privés.



Local investigation of the emissive properties of LaB₆–ZrB₂ eutectics

M.-H. Berger^{1,*} , T. C. Back^{2,3}, P. Soukiasian^{4,5}, D. Martinotti⁴, L. Douillard⁴, S. B. Fairchild³, J. J. Boeckl³, V. Filipov⁶, and A. Sayir^{7,8}

¹MINES ParisTech, PSL Research University, MAT - Centre des matériaux, CNRS UMR 7633, BP 87, 91003 Evry, France

²University of Dayton Research Institute, 300 College Park, Dayton, OH 45469-0170, USA

³Air Force Research Laboratory, Materials and Manufacturing Directorate, 3005 Hobson Way, Wright-Patterson Air Force Base, OH 45433, USA

⁴SPEC, CEA, CNRS, Université Paris-Saclay CEA Saclay, 91191 Gif Sur Yvette, France

⁵Université Paris-Sud, 91405 Orsay, France

⁶Frantsevitch Institute for Problems of Materials Sciences, National Academy of Sciences of Ukraine, Kiev, Ukraine

⁷NASA, Glenn Research Center, Cleveland, OH 44135, USA

⁸AFOSR, 801 N Randolph st, Arlington, VA 22203, USA

Received: 12 September 2016

Accepted: 17 January 2017

Published online:

30 January 2017

© Springer Science+Business Media New York 2017

ABSTRACT

LaB₆–ZrB₂ composites obtained by directional solidification at eutectic composition have been investigated by low-energy electron microscopy (LEEM) and thermal emission electron microscopy (ThEEM). The transitions from the mirror electron microscopy mode to the LEEM mode for the hexa- and diborides indicate lower work functions of the two phases when embedded in the composite compared to the corresponding single phases. In the composite, the work function of the ZrB₂ fibers is similar to that of the matrix and ThEEM images display a brighter contrast for the fibers. This is explained by the thermally activated diffusion of La on the fiber surface.

Introduction

Lanthanum hexaboride single crystals are widely used as electron emitters due to their low work function, their lower evaporation rate compared to refractory metals at thermionic emission temperatures, and their higher resistance to poisoning and ion bombardment. Due to these reasons, LaB₆ is one of the most widely used thermionic emission cathodes for a variety of applications and has been

particularly useful as hollow cathodes in Hall thrusters [1]. However, there are drawbacks with the material. LaB₆ is susceptible to thermal shock and this must be taken into account when determining operating parameters. Early on it was recognized the LaB₆ directionally solidified eutectics (DSEs) could offer improvements in mechanical stability while still preserving the electron emission properties of pure LaB₆ [2]. High-purity, defect-free LaB₆ DSE single crystals were produced by zone refining at the

Address correspondence to E-mail: marie-helene.berger@mines-paristech.fr

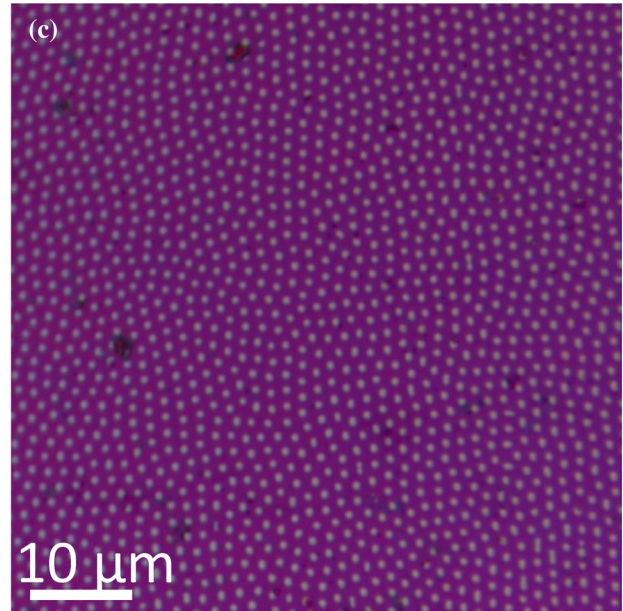
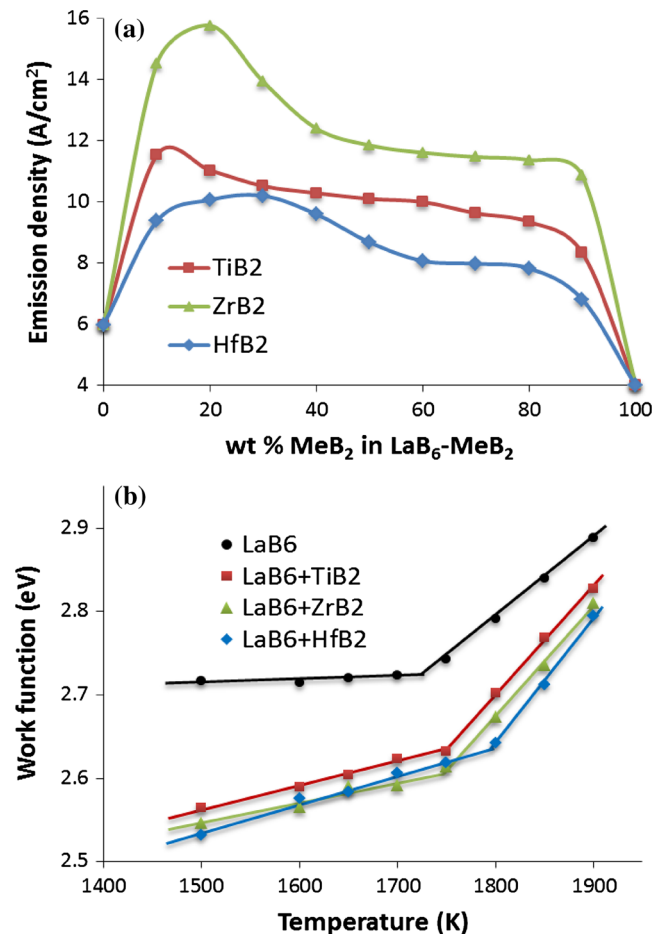


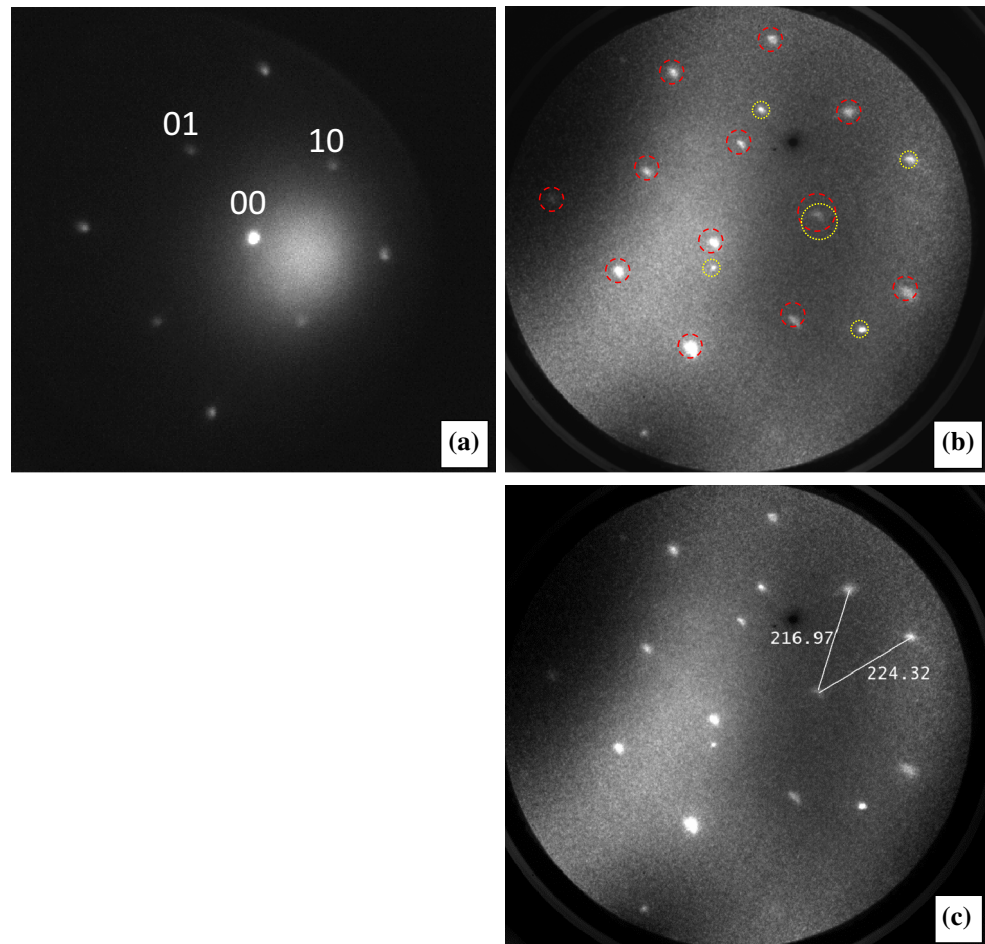
Figure 1 **a** Emission density at 1800 K of $\text{LaB}_6\text{-MeB}_2$ composites as a function of weight % addition of MeB_2 ($\text{Me} = \text{Zr}, \text{Ti}, \text{Hf}$). The maxima of emissivity are obtained at the eutectic compositions [9]. **b** Variation in temperature of the work function

of LaB_6 and of the three eutectics $\text{LaB}_6\text{-MeB}_2$ [9]. **c** Optical micrograph of the $\text{LaB}_6\text{-ZrB}_2$ composite at eutectic composition showing a regular distribution of ZrB_2 fibers in a LaB_6 matrix.

National Academy of Science of Ukraine from the 60s [3]. Investigation of alloying elements to improve the emission properties has been carried out in Pr Paderno's laboratory, which showed the non-solubility of *d*-transition metal atoms in the hexaboride and the formation of $\text{LaB}_6\text{-MeB}_2$ eutectics for metals of the IV column (Ti, Zr, Hf) [4]. Directional solidification at the eutectic compositions resulted in in situ composites made of a regular array of diboride fibers in a LaB_6 matrix. An improvement in the fracture toughness compared to LaB_6 was measured in these eutectics [5, 6], beneficial for their resistance to thermal cycling. Local investigation of their mechanical behavior showed crack deflection around the fibers [7, 8]. Differences in thermal expansion of the two constituents induce thermal residual stresses on cooling responsible for the interface driven composite effect. In addition, an increase in the emission current

density and a decrease in the work function compared to LaB_6 and to off-eutectic compositions could be measured [9], as illustrated in Fig. 1a, b. The highest emissive properties were obtained for $\text{Me} = \text{Zr}$ at the eutectic composition of 21% wt ZrB_2 and 79% wt LaB_6 . The physical mechanisms leading to the specific emissive behavior of the composite are not fully established. The hypothesis of an easier diffusion of lanthanum to the external surface through the $\text{LaB}_6/\text{ZrB}_2$ interfaces and fiber surfaces has been proposed [10]. An increased emissivity of the $\text{LaB}_6/\text{ZrB}_2$ interfaces due their distinct electronic structure, and the surrounding stress field has also been discussed. Hence, ab initio calculations applied to Cu(100) surfaces under different strain states revealed a clear dependence of the work functions to the strain [11]. The aim of this paper is to provide a local mapping of the emissive properties of the

Figure 2 LEED patterns of **a** the hexaboride matrix (001) surface and **b** the fiber (0001) surface. In addition to the hexagonal array of spots of ZrB_2 (red circles), a square array is observed (yellow circles). **c** Calibration of the pattern with the $1\bar{1}00$ of ZrB_2 (2.74 \AA) is used to determine the inverse distance between two yellow spots ($217 \text{ pixels} \times 2.74 \text{ \AA}/224 \text{ pixels} = 2.65 \text{ \AA}$). Within the precision of the diagram, the spots correspond to 200 of $\beta\text{-La}$ (fcc, $a = 5.30 \text{ \AA}$, $d_{200} = 2.65 \text{ \AA}$).



eutectic to identify the emissive areas and compare their work functions. These investigations have been achieved using low-energy and thermal emission electron microscopies (LEEM, TheEM) that provide the spatial resolution required to discriminate the matrix, interface, and fiber behaviors.

Materials and methods

The $\text{LaB}_6\text{-ZrB}_2$ eutectics and their parent single phases were solidified at the Frantsevitch Institute for Problems of Materials Sciences in Kiev using induction heating and a crucible-free zone melting process in argon atmosphere [3]. Disks of cross sections were mechanically polished to mirror finish. A typical optical image of the regular array of fibers obtained at the eutectic composition is shown in Fig. 1c. The samples were then introduced in the preparation chamber of the PEEM/LEEM (PEEM/LEEM III Elmitec GmbH at CEA-IRAMIS, Saclay) and

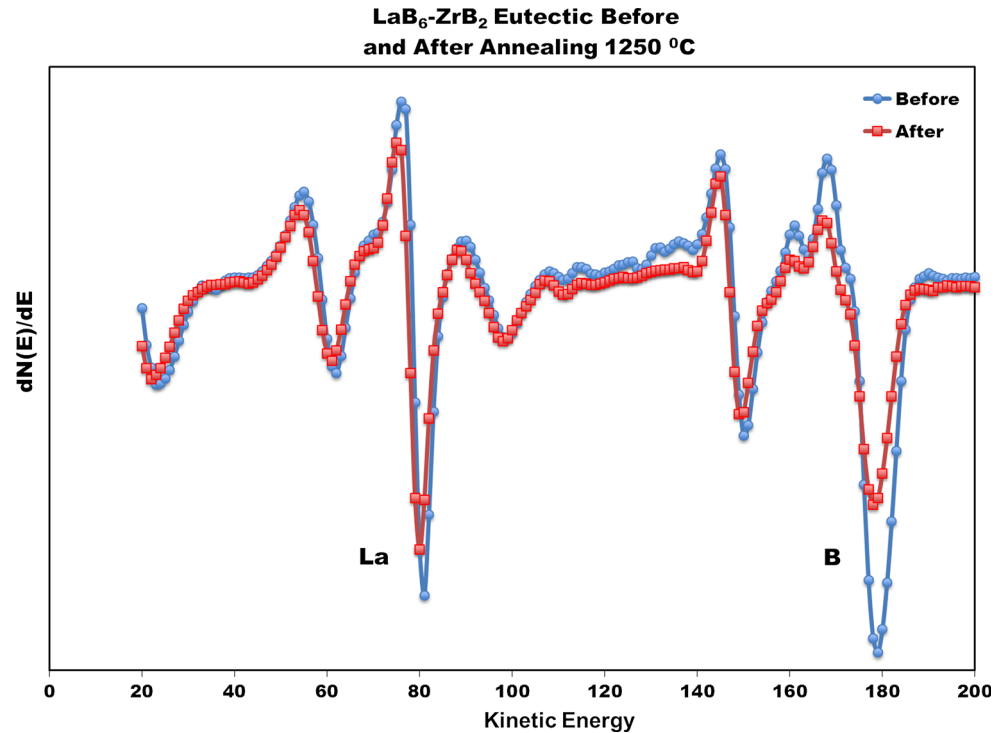
annealed at 10^{-7} mbar and $1250 \text{ }^\circ\text{C}$ for 10 min to clean the surface and remove surface oxides. The as-prepared eutectics were directly transferred into the ultra-high vacuum (10^{-10} mbar) of the PEEM/LEEM chamber.

Results

Structure of the surfaces—LEED and Auger analyses

Low-energy electron diffraction patterns were first recorded on the matrix to check the surface quality. If a thin amorphous oxide layer were covering the sample, no periodic pattern would be obtained. The pattern displayed in Fig. 2a shows the crystallinity of the (001) surface (LaB_6 : cubic $\text{Pm}\bar{3}m$, $a = 0.4157 \text{ nm}$). LEED patterns recorded on the fibers display hexagonal array of spots (red larger circles) typical of (0001) ZrB_2 surface (ZrB_2 : hexagonal, $\text{P6}/\text{mmm}$,

Figure 3 Auger electron spectroscopy of $\text{LaB}_6/\text{ZrB}_2$ surface before and after annealing. After annealing shows an increase in La relative to B, which supports La diffusion model previously proposed.



$a = 0.3169 \text{ nm}$ $c = 0.3530 \text{ nm}$) (Fig. 2b). These diffraction patterns obtained on transverse cross sections of the eutectic show that the \vec{c} axes of the two phases are almost parallel and close to the solidified rod axis. This is consistent with previous TEM and XRD analyses [8, 12]. An additional set of spots is observed (yellow circles forming a deformed square) that cannot be assigned to LaB_6 matrix but could result from (001) plane of the β -La (cubic Fm $\bar{3}m$ $a = 0.5304 \text{ nm}$). β -La is a high-temperature allotropic form seen from $\sim 300 \text{ }^\circ\text{C}$ that can be stabilized down to room temperature by impurities [13]). This is well supported by Auger data. Figure 3 shows before and after results of thermal anneal cycle. It can clearly be seen that after annealing the La/B ratio has increased. These results suggest that an excess of La is present on the surface.

Quantitative differences in their work functions—MEM/LEEM transition

A series of images were recorded at room temperature to determine the mirror electron microscopy (MEM) mode/LEEM mode transition [14], [15]. The sample is biased to a negative potential close to that of the LEEM electron gun (-20 kV). The potential difference between the sample and the gun is termed

start voltage (SV) and was varied from -5 to 5 V by increments of 0.1 V . Representative images are displayed in Fig. 4. At the lowest negative values of SV, the primary electrons cannot penetrate the sample, which is known as mirror mode. In mirror mode, electrons are reflected on an equipotential surface just above the sample surface. The image intensity is high and shows a plateau or increases slightly when SV is gradually increased, up to a threshold value at which the intensity drops abruptly. At this voltage SV_0 , the vacuum energy levels of the gun equals that of the sample and electrons can be injected into the sample and a weak back scattered electron signal is obtained. When SV is increased above SV_0 , the image intensity increases as more electrons are back scattered, see Fig. 5. SV_0 represents the difference in work function between the sample and the electron source. As the work function of the source is constant, larger SV_0 indicates higher work function of the probed phase. Moreover, if the two phases do not have the same work functions, the drops of intensity are not seen at the same start voltages.

The mean intensities in the matrix and in the fibers have been calculated for each start voltage using a series of masks applied separately on the two phases. The variations of the obtained intensities as a function of the start voltage are shown in Fig. 5 for ZrB_2

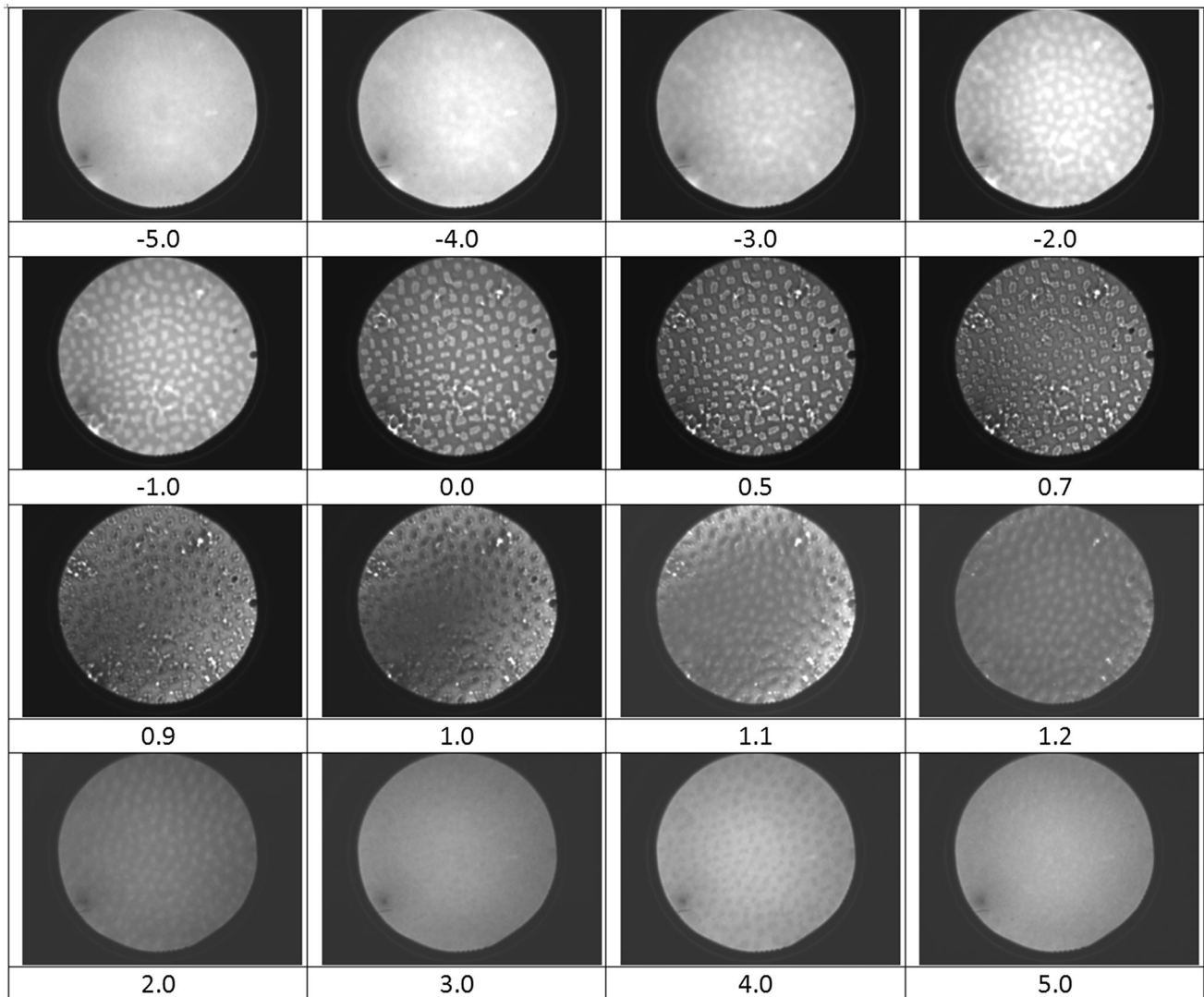


Figure 4 Representative MEM/LEEM images recorded at room temperature for increasing start voltages from -5 volts to 5 volts. For an easier visualization, the mean contrasts have been normalized. Starting from -5 V (MEM mode), the absolute intensity is increasing slightly up to 0.9 V where it starts to

and LaB_6 in the eutectic. Figure 5 shows a drop of intensity at ~ 0.9 V for the fibers and ~ 1.1 V for the matrix. The same methodology has been followed for the pure parent phases, LaB_6 and ZrB_2 , and the corresponding curves are also shown in Fig. 5 to compare the threshold values given by these four curves. The main information is that the work functions of the two phases are significantly lower (~ -0.4 eV) when embedded in the composite than as single phases. In addition, if the work function of ZrB_2 is higher than that of LaB_6 in the single phases, it seems slightly lower in the composite.

decrease (to LEEM mode). At 0.9 V, the fibers become darker than matrix. The contrast is reversed at 1.1 V. This earlier drop of the fibers intensity than the matrix intensity could be explained by a lower work function for the diboride.

Thermal emissivity—ThEEM maps

To map the variation of thermal emissivity across the section of the composite, the sample was heated to 750°C , the electron gun of the LEEM switched off and an electronic image was built from the electrons thermally emitted. The corresponding ThEEM images are shown in Fig. 6. In this imaging mode, no electron or photon source is used. Only thermally emitted electrons are used for imaging. Consequently, the brightest areas in the image will represent areas with the lowest work function. It is clearly

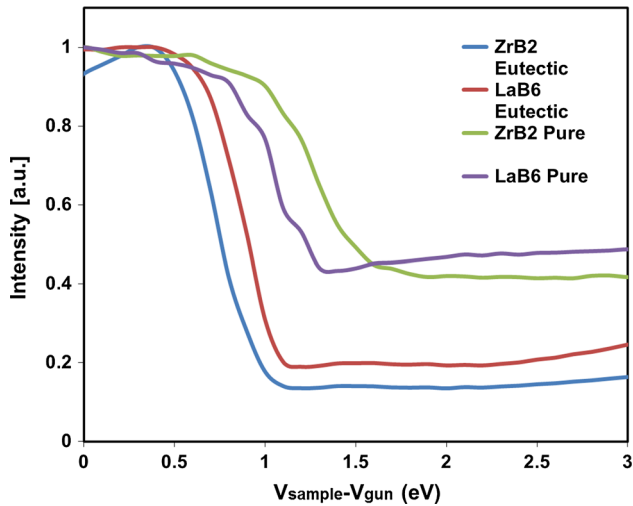


Figure 5 Variation of the mean intensity in LaB_6 and ZrB_2 phases in the MEM/LEEM images as function of the start voltage around the MEM/LEEM transition. As the constant reference work function of the source is not precisely known, the curves indicate the relative values of the work functions of the phases. The start voltage is increased by 0.5 V between two x axis ticks.

seen that the brightest areas are located on/around the ZrB_2 phase compared to the LaB_6 matrix phase. (0001) ZrB_2 has a work function of ~ 4.7 eV [16] and should not emit before the (001) LaB_6 matrix phase with a work function ~ 2.7 eV [17]. Two possible explanations exist that could result in the lowering of the work function on the ZrB_2 phase. The first explanation for this is the strain state in the material. It was previously shown that the ZrB_2 in the $\text{LaB}_6/\text{ZrB}_2$ DSE exists in a state tension due differences in coefficients of thermal expansion [5] [18]. Tensile

stress has been shown to decrease the work function of Cu (100) surface [11]. It is possible that a similar effect is occurring with the eutectic. The second explanation could be surface diffusion of La metal on the diboride phase creating the optimal dipole arrangement for lowering the work function barrier. Although neither mechanism can be ruled out, a La diffusion mechanism is well supported by LEED and Auger data.

Discussion

A decrease of ~ 0.4 eV of the work function of the composite compared to hexaboride single crystal is measured in these room temperature MEM/LEEM transition experiments. This confirms the better emissive behavior of the eutectic announced by the Pr Paderno's group. The local investigations by LEEM and THEEM of this work have elucidated the role of the fibers in the composite behavior. The diboride work function is significantly reduced when incorporated in the LaB_6 matrix (MEM/LEEM transition). The LEED patterns of the fibers suggest their partial coverage by La. Lanthanum vapor pressure at 1050 °C of La is about $3 \cdot 10^{-8}$ mbar which is more than 5 orders of magnitude higher than that of B and Zr [19]. The annealing step carried out before the LEEM characterization at 1250 °C to remove surface oxides might have induced an evaporation or diffusion of La, partially covering the fiber surfaces. The La richer surface layers explain the brightest contrast observed on the fibers in THEEM. The scenario

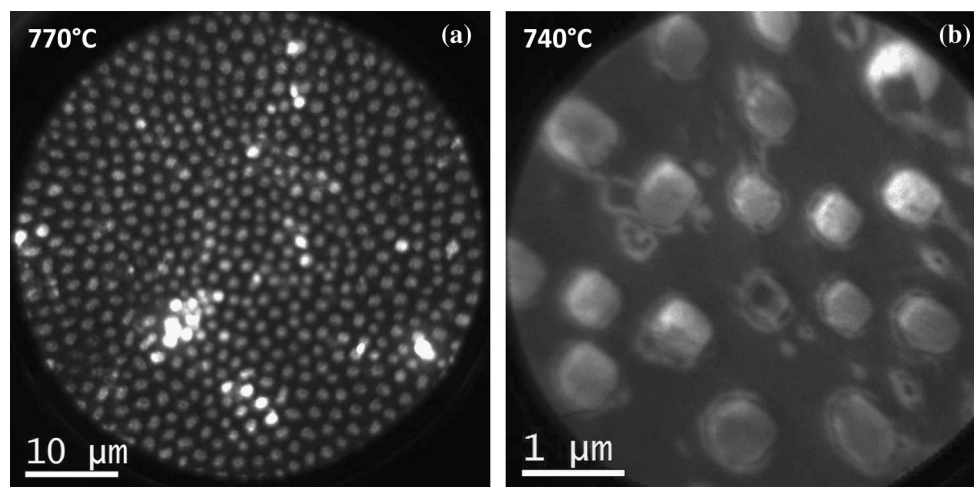


Figure 6 Thermal emission images of the composite at **a** 770 °C and **b** 740 °C, showing a brighter contrast for the fibers.

proposed by Pr Paderno's group is validated. An additional effect of the tensile strain field on the fibers is expected.

Acknowledgements

M. H. Berger and T. C. Back would like to acknowledge support from the Air Force Office of Scientific Research (AFOSR). TC Back would also like to acknowledge Prof. Martin Kordesch for useful discussions.

References

- [1] Goebel DM, Chu E (2013) High-current lanthanum hexaboride hollow cathode for high-power hall thrusters. *J Propuls Power* 30:35–40
- [2] Niemyski T, Pracka I, Jun J, Paderno J (1968) On zone melting of alkaline and rare-earth metal hexaboride rods. *J Common Met* 15:97–99
- [3] Paderno YB, Lazorenko VI, Kovalev AV (1981) Zone refining and growth of lanthanum hexaboride single crystals. *Powder Metall Met Ceram* 20:717–721
- [4] Ordan'yan SS, Paderno YB, Khoroshilova IK et al (1983) Interaction in the $\text{LaB}_6\text{-ZrB}_2$ system. *Powder Metall Met Ceram* 22:946–948
- [5] Paderno YB, Paderno V, Filippov V et al (1992) Structure features of the eutectic alloys of borides with the d-and f-transition metals. *Powder Metall Met Ceram* 31:700–706
- [6] Paderno YB, Paderno VN, Filippov VB (2000) Directionally crystallized ceramic fiber-reinforced boride composites. *Refract Ind Ceram* 41:373–378
- [7] Paderno YB (1998) A new class of "In-Situ" fiber reinforced boride composite ceramic materials. In: Haddad YM (ed) *Proceedings of the NATO advanced research on Multilayered and Fibre-Reinforced Composites : Problems and Prospects*. Kluwer Academic Publishers, Kiev, Ukraine, pp 353–369, 2-6 June, 1997. <http://www.springer.com/us/book/9780792349112>
- [8] Deng H, Dickey EC, Paderno Y et al (2004) Crystallographic characterization and indentation mechanical properties of $\text{LaB}_6\text{-ZrB}_2$ directionally solidified eutectics. *J Mater Sci* 39:5987–5994. doi:10.1023/B:JMSC.0000041695.40772.56
- [9] Paderno Y, Paderno V, Filippov V (1994) Crystal chemistry of eutectic growth of d-and f-transition metals borides. *JJAP Ser 10*:190–193
- [10] Taran A, Voronovich D, Plankovskyy S et al (2009) Review of LaB_6 , Re-W dispenser, and $\text{BaHf O}_3\text{-W}$ cathode development. *IEEE Trans Electron Devices* 56:812–817. doi:10.1109/TED.2009.2015615
- [11] Wang XF, Li W, Lin JG, Xiao Y (2010) Electronic work function of the Cu (100) surface under different strain states. *EPL Europhys Lett* 89:66004. doi:10.1209/0295-5075/89/66004
- [12] Jouanny I, Sennour M, Berger MH et al (2014) Effect of Zr substitution by Ti on growth direction and interface structure of $\text{LaB}_6\text{-Ti}_x\text{Zr}_{1-x}\text{B}_2$ directionally solidified eutectics. *Dir Solidified Eutectics Sel Pap DSEC IV* 34:2101–2109. doi:10.1016/j.jeurceramsoc.2014.01.026
- [13] Spedding F, Hanak J, Daane A (1961) High temperature allotropy and thermal expansion of the rare-earth metals. *J Common Met* 3:110–124
- [14] Babout M, Guittard C, Guivarch M et al (1980) Mirror electron microscopy applied to the continuous local measurement of work-function variations. *J Phys Appl Phys* 13:1161
- [15] Anderson ML, Nakakura CY, Kellogg GL (2009) Imaging doped silicon test structures using low energy electron microscopy. Sandia Rep. SAND2009-7981. <http://prod.sandia.gov/techlib/accesscontrol.cgi/2009/097981.pdf>
- [16] Tomida Y, Nitta S, Kamiyama S et al (2003) Growth of GaN on ZrB_2 substrate by metal-organic vapor phase epitaxy. *Appl Surf Sci* 216:502–507. doi:10.1016/S0169-4332(03)00466-5
- [17] Swanson L, Gesley M, Davis P (1981) Crystallographic dependence of the work function and volatility of LaB_6 . *Surf Sci* 107:263–289
- [18] Deng H (2006) Study of the interface behavior in directionally solidified $\text{LaB}_6\text{-ZrB}_2$ eutectics. Ph.D. dissertation, PennState University
- [19] Honig RE (1962) Vapor pressure data for the solid and liquid elements. *RCA Rev* 23:567–586